A Two-Dimensional Surf Zone Model
Based on the Boussinesq Equations

H.A. Schäffer[1], R. Deigaard[2] and P. Madsen[1]

Abstract

A simple approach to wave breaking using the concept of surface rollers is intro-
duced in a two-dimensional Boussinesq model. A surface roller represents a passive
bulk of water riding on the front of a breaking wave and the vertical redistribution
of momemtum associated with the formation and change of surface rollers leads to
additional terms in the Boussinesq equations. A simple geometrical method is used
for the determination of the shape and location of these rollers at each time step in
the simulation. This automatically results in a time-varying break point position in
the case of irregular waves. Furthermore, breaking may well cease for example
when waves reach a trough inshore of a bar.
  Comparison between one-dimensional simulations and experiments shows
good agreement for the variation of wave height and mean water surface as well as
surface elevation time series throughout the surf zone for both regular and irregular
waves. Simulations in two horizontal dimensions are still at the initial stage. A
sample simulation is shown.

Introduction

The modelling of wave conditions in the surf zone is an important basis for the
description of wave-driven currents and sediment transport.
  Previously, waves breaking on a beach have been modelled by the non-
linear shallow water equations. These predict that the front face of the wave will
gradually become steeper until it is vertical. In such a model, the front of a break-

---

[1] Danish Hydraulic Institute, Agern Allé 5, 2970 Hørsholm, Denmark

[2] DTH, ISVA, DK-2800 Lyngby, Denmark

ing wave may then be represented by a jump condition in which mass and momentum are conserved. Thus only the integrated energy dissipation over the wave front is represented.

The details of the turbulent front of a bore were studied by Madsen (1981) and Madsen and Svendsen (1983) and Svendsen and Madsen (1984) using a two-layer model, and it was found that the energy dissipation can be represented in a depth-integrated model by taking the non-uniform velocity distribution into account in the momentum equation.

The main restrictions for the use of the non-linear shallow water equations are that they can only be used for very shallow water, and that they cannot describe a wave of constant form propagating over an even bottom. One consequence of this is that the offshore boundary must be very close to the surf zone and in some cases even within the surf zone. Another consequence is that once a wave has started breaking, it will continue to do so even if it enters deeper water, eg in a trough inshore of a bar. Due to these restrictions, it is of interest to develop a model for the surf zone based on the Boussinesq equations which has a wider range of applicability than the non-linear shallow water equations.

Boussinesq models for the surf zone have been developed by Abbott et al (1983), Karambas and Koutitas (1989, 1992) and Karambas et al (1990) using a depth-integrated one-or-two-equation turbulence model. Deigaard (1989) introduced the concept of surface rollers in Boussinesq modelling and estimated the surface roller geometry using ideas of Engelund (1981). The roller was taken to be a lump of water moving with the speed of wave propagation as in the models of Svendsen (1984, 1984a). The present work is an extension and modification of the model by Deigaard (1989).

The Flow Description

The flow velocity in the surface roller is very large compared to the orbital motion, as the water in the roller travels with the wave celerity, c. Thus, the velocity distribution is very uneven in the presence of rollers. The breaking/broken waves are represented by including the effect of the surface rollers in the equations expressing the conservation of mass and momentum. The contribution from the rollers is determined by considering the momentum flux of the velocity profile shown in Figure 1. First, the one-dimensional case is considered. The orbital velocity, U_o, is taken to be uniformly distributed over the vertical, and the surface roller with a thickness δ has the velocity c. The instantaneous water depth is h, the still water depth is D, and the water surface elevation is η.

The instantaneous depth-integrated flux in the x-direction p is then

$$p = \int_{-D}^{\eta} u \, dz = U_o \, (h-\delta) + c \, \delta = U_o \, h + (c - U_o) \, \delta \qquad (1)$$

and the depth-integrated momentum flux, F_m, is

$$F_m = \int_{-D}^{\eta} \rho \, u^2 \, dz = \rho \, U_o^2 \, (h-\delta) + \rho \, c^2 \, \delta \qquad (2)$$

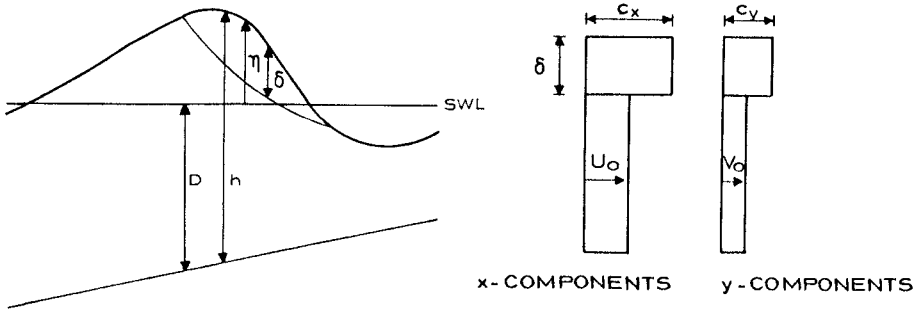$$= \rho \, U_o^2 \, h + \rho \, (c^2 - U_o^2) \, \delta$$

Figure 1.   Cross-section and assumed velocity profile components of a breaking wave with a surface roller.

If no roller is present ($\delta = 0$), the momentum flux of the uniformly-distributed orbital velocity is given by

$$F_{mo} = \rho \, \frac{p^2}{h} \qquad (3)$$

Retaining this expression for the momentum flux, even when rollers are present, a correction term must be included. This term (divided by ρ) takes the form

$$R = \frac{1}{\rho} \, (F_m - F_{mo})$$

$$= U_o^2 \, h + (c^2 - U_o^2) \, \delta \, - \frac{1}{h} \, (U_o \, h + (c-U_o) \, \delta)^2 \qquad (4)$$

$$= \delta \, (c-U_o)^2 \left(1 - \frac{\delta}{h}\right)$$

or with U_o determined from (1):

$$R = \delta \left(\frac{ch-p}{h-\delta}\right)^2 \left(1 - \frac{\delta}{h}\right) = \delta \frac{\left(c - \frac{p}{h}\right)^2}{1 - \frac{\delta}{h}} \qquad (5)$$

This contribution to the momentum flux from the rollers is then - together with F_{mo} - included in the full Boussinesq equation for conservation of momentum:

$$\frac{\partial p}{\partial t} + \frac{\partial}{\partial x}\left(\frac{p^2}{h}\right) + \frac{\partial R}{\partial x} + gh\,\frac{\partial \eta}{\partial x} + \frac{D^3}{6}\,\frac{\partial^3}{\partial x^2 \partial t}\left(\frac{p}{D}\right) - \frac{D^2}{2}\,\frac{\partial^3 p}{\partial x^2 \partial t} = 0 \qquad (6)$$

The continuity equation is not affected by the presence of rollers:

$$\frac{\partial \eta}{\partial t} + \frac{\partial p}{\partial x} = 0 \qquad (7)$$

When the flow equations are solved with the surface rollers at the wave fronts, the additional, third term in the momentum equation will cause an energy loss, which represents the energy dissipation in spilling breakers and broken waves.

The extension of this analysis to two dimensions is simple, and the three correction terms R_{xx}, R_{xy} and R_{yy} are given by the expressions:

$$\frac{1}{\rho}\,F_{mxx} = \int_{-D}^{\eta} u^2\,dz = \frac{p^2}{h} + \delta\,\frac{\left(c_x - \dfrac{p}{n}\right)^2}{1 - \dfrac{\delta}{h}} = \frac{p^2}{h} + R_{xx} \qquad (8)$$

$$\frac{1}{\rho}\,F_{mxy} = \int_{-D}^{\eta} uv\,dz = \frac{pq}{h} + \delta\,\frac{\left(c_x - \dfrac{p}{h}\right)\left(c_y - \dfrac{q}{h}\right)}{1 - \dfrac{\delta}{h}} = \frac{pq}{h} + R_{xy} \qquad (9)$$

$$\frac{1}{\rho}\,F_{myy} = \int_{-D}^{\eta} v^2\,dt = \frac{q^2}{h} + \delta\,\frac{\left(c_y - \dfrac{q}{h}\right)^2}{1 - \dfrac{\delta}{h}} = \frac{q^2}{h} + R_{yy} \qquad (10)$$

where c_x and c_y are the x- and y-components of the wave celerity vector, and q is the depth-integrated flux in the y-direction. $\partial R_{xx}/\partial x + \partial R_{xy}/\partial y$ is then included in the equation for x-momentum and $\partial R_{yy}/\partial y + \partial R_{xy}/\partial x$ is included in the equation for y-momentum. The equation for mass conservation is unchanged:

$$\frac{\partial \eta}{\partial t} + \frac{\partial p}{\partial x} + \frac{\partial q}{\partial y} = 0 \qquad (11)$$

Geometrical Determination of Surface Rollers

The consequence of the presence of surface rollers has now been established and it remains to determine their variation in space and time, $\delta(x,y,t)$. There is no appropriate theory available for this purpose, and we adapt the heuristic geometrical approach of Deigaard (1989) with some modifications.

As a shoaling wave approaches a shoreline, the local steepness of the front increases, the wave becomes unstable, and breaking initiates. Assuming that the local gradient of the front of a non-breaking wave has a maximum $\tan\varphi$, we simply take the wave to be breaking when this gradient is exceeded. Furthermore, we assume that the water above the tangent of slope $\tan\varphi$, to the water surface belongs to the roller as shown in Figure 2. This also implies that breaking ceases if the maximum of the local slope becomes less than $\tan\varphi$.
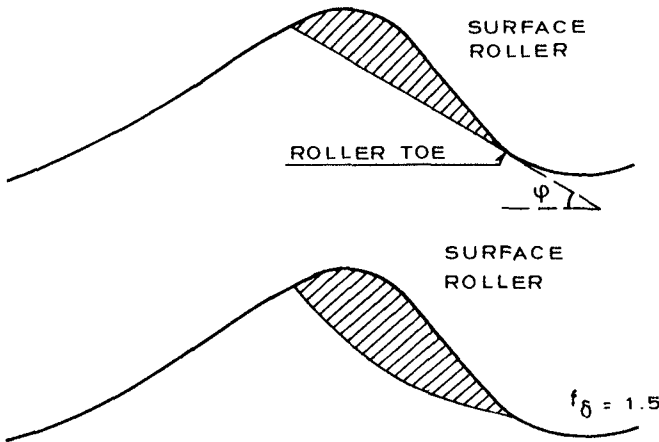

Figure 2.   a: Geometrical detection of surface roller (cross-section A-A in Figure 3), b: The same roller with $f_\delta = 1.5$ applied.

Engelund (1981) found that $\varphi = 10°$ was appropriate for weak hydraulic jumps, and using the bore/hydraulic jump analogy, we use this value in the inner surf zone. However, waves over a constant depth can be stable for much larger local slopes from which it is clear that $\varphi = 10°$ is inadequate near the break point. For this reason, φ is chosen to vary in time while being constant in space within each surface roller.

Breaking is initiated using $\varphi = \varphi_B$, which then gradually changes to the smaller terminal value $\varphi = \varphi_o$. Since breakers often transform rather quickly to the bore-like stage, an exponential transition of $\tan\varphi$ is chosen:

where t* is the halftime for $(\tan\varphi - \tan\varphi_o)$. Thus, the roller is determined by the three parameters, $\tan\varphi_B$, $\tan\varphi_o$, and t*.

Furthermore, we introduce a roller shape parameter, f_δ, to partially com-

$$\tan\varphi = \tan\varphi_o + (\tan\varphi_B - \tan\varphi_o) \exp\left[- \ln2 \; \frac{t-t_B}{t*}\right] \qquad (12)$$

pensate for the primitive way of separating the surface roller from the rest of the flow. After the geometrical determination of the roller at each time step, δ is simply multiplied by f_δ before the influence of the roller is computed. Note that this has no direct influence on the roller determination.

In the 2D case, the toe of the roller becomes a curve (segment) instead of a single point, see Figure 3, and the cut-off line is a surface defined by the roller-toe curve and a set of generating lines. These generating lines are determined by the instantaneous local cut-off angle, φ, and the local direction of the maximum slope of the free surface.
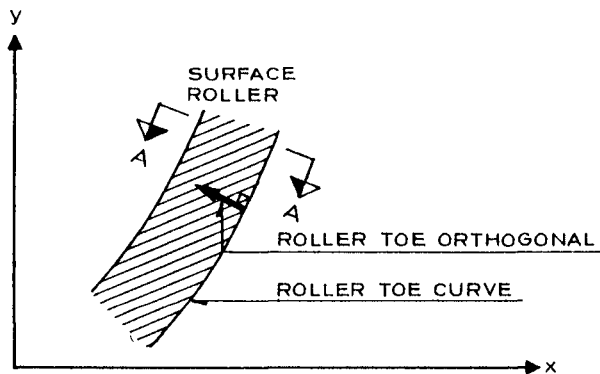

Figure 3.   *Plane view of a 2D surface roller. The cross vertical section A-A is shown in Figure 2.*

The roller shape parameters, f_δ, is maintained without difficulty. As in the 1D case, φ (tan φ to be exact) is chosen to vary as given by (12). In the 2D case, however, φ is not constant in space within each surface roller (as in the 1D case), but only along a roller-toe orthogonal (see Figure 3), ie a lateral variation of φ within each roller is possible. This is because the age of different sections of the surface roller may vary: from the time of initial breaking, each roller section is traced along the roller-toe orthogonal and this provides a way of determining the age of each roller section. This age is then used for the determination of the local value of φ.

The detection procedure outlined above automatically allows for very different situations within the same surface roller. For example, for oblique incident waves on a beach, the bore-like stage in the inner surf zone is modelled using $\varphi = \varphi_0$ simultaneously with initial breaking ($\varphi \approx \varphi_B$) occurring in the seaward end of the roller.

Numerical Results and Comparison with Measurements

In all numerical simulations shown below, three of the four parametres governing the instantaneous determination of the surface roller were kept constant using $\varphi_o = 10°$, $t^*/T_{(p)} = 0.1$ where $T_{(p)}$ is the (peak) period, and $f_\delta = 1.5$. Furthermore, $\varphi_\beta = 20°$ was used in all tests but one, for which it was necessary to reduce the value to $\varphi_\beta = 18°$ in order to match the measured break point. At the seaward boundary, the depth-integrated velocity was specified, and at the shoreward boundary, the remaining waves were absorbed by a numerical sponge layer (Larsen and Dancy, 1983). The celerity was modelled by $1.3\sqrt{gD}$ throughout.

Figure 4a shows the surface elevation at $t = 24$ s including the rollers for a regular wave of $T = 4$ s climbing a plane slope of 1:40. This computation was made with a time step of 0.1 s and a grid size of 0.4 m, using 37 CPU seconds on an IBM 4381 P12. The figure gives a first impression of the capability of the model to reproduce the wave decay and the development of asymmetric wave profiles resembling bores. Figure 4b shows the results when no surface-roller term is applied.
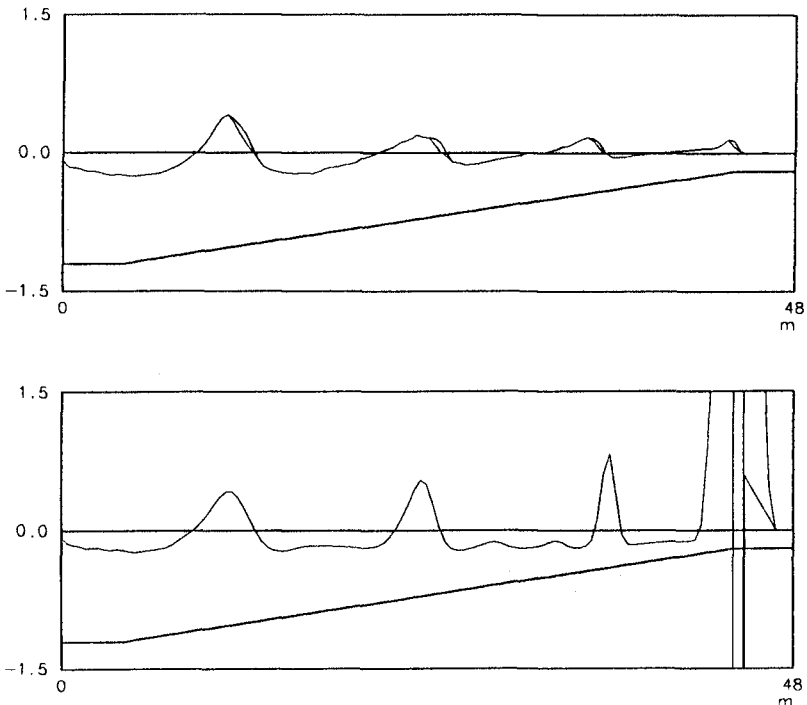

Figure 4.   *Instantaneous surface elevation of regular waves on a plane sloping beach. a: with surface rollers, b: without surface rollers.*

In Figure 5, comparison of wave height, H, and mean water surface, MWS, with measurements from DHI (Thorkildsen et al, 1991) is shown. The beach profile has a bar with a depth of 0.10 m and the waves are regular with T = 1.6 s and H_o = 0.12 m (wave height at seaward boundary where the depth is 0.54 m).
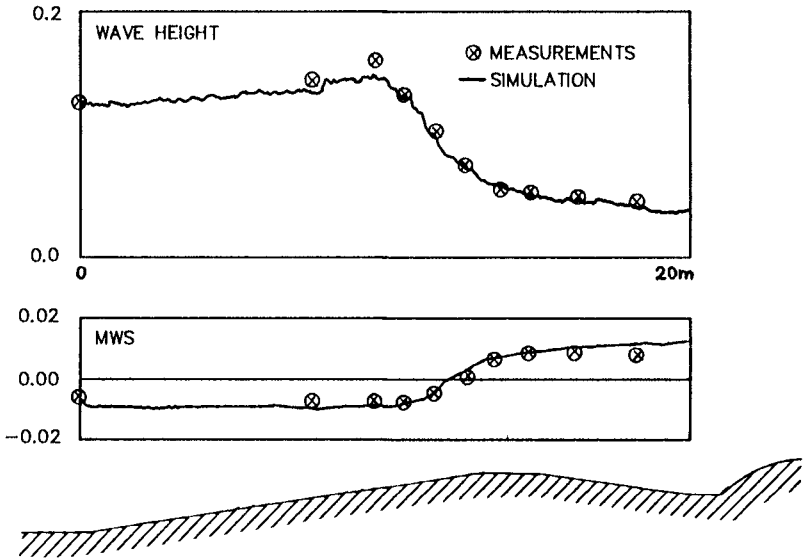

Figure 5.   Comparison of wave height and mean water surface with DHI measurements for regular waves breaking over a bar (Thorkildsen et al, 1991).

Both the wave height and MWS compare very well with measurements. An interesting feature is that both measurements and numerical results exhibit the well-known 'delay' of the change of sign for the MWS-gradient relative to the break point. This indicates that the model reproduces the effect of a rapid transformation of potential energy to kinetic energy and the change in the wave profile taking place in the initial breaking process. In Figure 6, surface elevation time series for another profile with a bar are compared with measurements from Hansen and Svendsen (1986). At the two locations shown, the depth was 70% and 42% of the breaker depth, respectively. The latter location is on the top of the bar where breaking has almost ceased, and the wave height is seen to be somewhat overestimated.
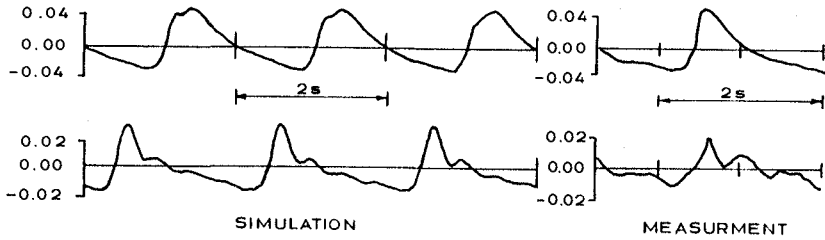
Figure 6.   *Comparison of surface elevation time series with measurements by Hansen and Svendsen, 1986.*

We now turn to irregular waves bearing in mind that this only requires a change in the seaward boundary condition for the simulation and that no additional assumptions are needed regarding eg the variation of the break point position. Figures 7, 8 and 9 show results for incoming waves given by a JONSWAP spectrum with random phase assignment and a peak enhancement factor of 3.3. The incoming significant wave height is 0.14 m and the peak period is 1.8 s. The profile is the same as for the results shown in Figure 5 (Thorkildsen et al, 1991).

Figure 7 shows an instantaneous surface elevation and Figure 8 gives spatial variation of the RMS of the surface elevation as well as the MWS. Both quantities compare well with measurements, except for a general vertical shift between calculated and measured MWS-values. This, however, is explained by loss of water in the numerical sponge layer due to setup, and the problem is expected to disappear when a run-up condition is incorporated. Figure 9 shows time series of surface elevation at gauges nos 5 and 9 (indicated in Figure 8). The agreement is surprisingly good considering that the physical and numerical shoreline absorption are bound to be a little bit different.
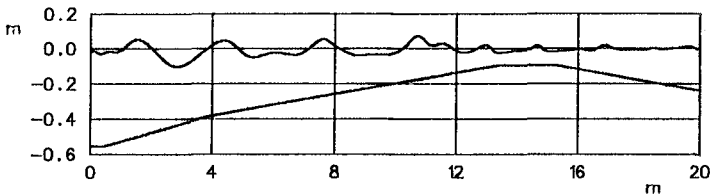

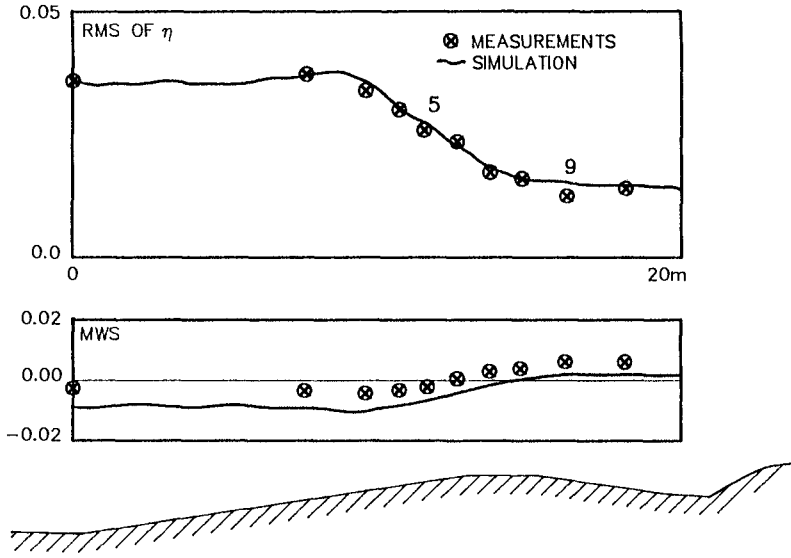*Figure 7.*   *Instantaneous surface elevation of irregular waves breaking over a bar.*

Figure 8.   *Comparison of RMS of surfave elevation and mean water*
                   surface for irregular waves breaking over a bar with DHI
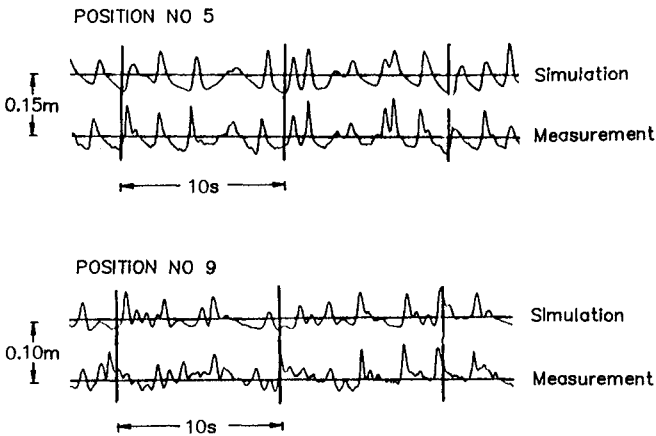   *measurements (Thorkildsen et al, 1991).*

Figure 9.   *Comparison of time series of surface elevation for posi-*
                   tions nos 5 and 9 in Figure 8.

Figure 10 shows a close-up of the instantaneous surface roller thickness and surface elevation for a two-dimensional simulation of a regular wave ($H_o = 0.15$ m, $T = 2$ s) breaking over a focusing shoal. The topography, known as the Whalin shoal, is given in Figure 11 where the close-up area is indicated by the square. The effects of breaking (Figure 10) have resulted in a decay of wave height in the central part of the wave. Without breaking, this part of the wave would have been the highest.
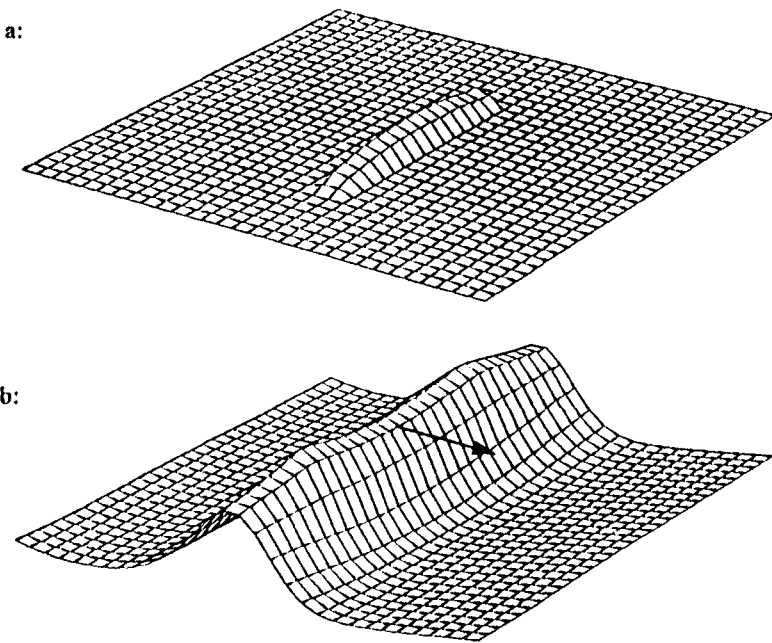

Figure 10.   Two-dimensional simulation of a wave breaking over a focusing shoal. a: surface roller, b: surface elevation.
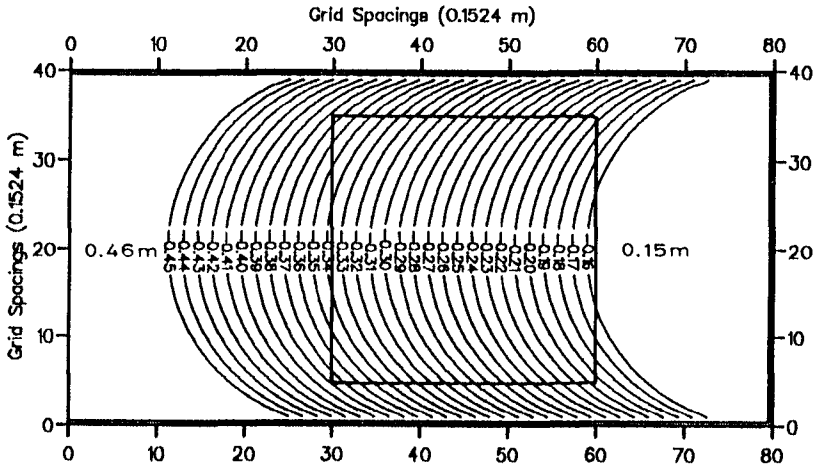
Grid Spacings (0.1524 m)

Figure 11.   *Focusing shoal (Whalin topography).*

Conclusion

Effects of wave breaking have been successfully incorporated in a Boussinesq model using the concept of surface rollers. Comparison with experiments shows that the model is capable of reproducing the variation of wave height and mean water surface for regular as well as irregular waves breaking in shallow water. Even details of surface elevation time series in the inner surf zone are reproduced quite well. The model has the potential to simulate irregular short-crested waves over a varying topography under surf conditions including phenomena like nearshore calculation and infragravity waves.

Acknowledgements

References

Abbott, M.B., J. Larsen, P. Madsen, and J. Tao (1983), *'Simulation of wave breaking and run-up'*. Seminar on hydrodynamics of waves in coastal areas, Moscow, September 1983. Arranged by International association for hydraulic research in connection with the 20th congress of IAHR, Moscow, September 1983.

Deigaard, R. (1989), *'Mathematical modelling of waves in the surf zone'*. Progress Report 69, pp 47-59. ISVA, Technical University, Lyngby, Denmark.

Engelund, F. (1981), *'A simple theory of weak hydraulic jumps'*, Progress Report 54, pp 29-32. ISVA, Technical University, Lyngby, Denmark.

Hansen, J.B. and I.A. Svendsen (1986), *'Experimental investigation of the wave and current motion over a longshore bar'*. Proceedings 20th Int. Conf. Coastal Engineering, Taiwan, Vol 2, pp 1166-1179.

Karambas, Th., Y. Krestenitis, and C. Koutitas (1990), *'A numerical solution of Boussinesq equations in the inshore zone'*. Hydrosoft, Vol 3, No 1, pp 34-37.

Karambas, Th. and C. Koutitas (1990), *'Mathematical modelling of short waves in surf zone'*. In Water Wave Kinematics. A. Tørum and O.T. Gudmestad (eds), Kluwer Academic Publishers, pp 351-365.

Karambas, Th. and C. Koutitas (1992), *'A breaking wave propagation model based on the Boussinesq equations'*. Coastal Enginering, Vol 18, pp 7-20.

Larsen, J. and H. Dancy (1983), *'Open boundaries in short wave simulations - a new approach'*. Coastal Engineering, Vol 7, No 3, pp 285-297.

Madsen, P.A. (1981), *'A model for a turbulent bore'*. Ph.D. thesis, Series paper 28, ISVA, Technical University, Lyngby, Denmark.

Madsen, P.A. and I.A. Svendsen (1983), *'Turbulent bores and hydraulic jumps'*. Journal of Fluid Mechanics, Vol 129, pp 1-25.

Svendsen, I.A. and P.A. Madsen (1984), *'A turbulent bore on a beach'*. Journal of Fluid Mechanics, Vol 148, pp 73-96.

Svendsen, I.A. (1984), *'Wave heights and setup in a surf zone'*. Coastal Engineering, Vol 8, no 4, pp 303-329.

Svendsen, I.A. (1984a), *'Mass flux and undertow in a surf zone'*. Coastal Engineering, Vol 8, no 4, pp 347-365.

Thorkildsen, M., N. Rosing, and H.A. Schäffer (1991), *'Experimental investigation of waves breaking over a bar'*. Extended abstract. Proc. of Mid-Term Workshop of the MAST G6-M Project, Edinburgh, September 1991.